Journal of Zhejiang University-SCIENCE A (Applied Physics & Engineering)
ISSN 1673-565X (Print); ISSN 1862-1775 (Online)
www.zju.edu.cn/jzus; www.springerlink.com
E-mail: jzus@zju.edu.cn

On the role of the constitutive model and basal texture on the mechanical behaviour of magnesium alloy AZ31B sheet*

H. WANG[1], P. D. WU[†‡1], K. W. NEALE[2]

([1]*Department of Mechanical Engineering, McMaster University, Hamilton, Ontario L8S 4L7, Canada*)

([2]*Faculty of Engineering, University of Sherbrooke, Sherbrooke, Quebec J1K 2R1, Canada*)

[†]E-mail: peidong@mcmaster.ca

Received Mar. 19, 2010; Revision accepted June 17, 2010; Crosschecked Aug. 26, 2010

Abstract: The recently developed elastic-viscoplastic self-consistent model with various self-consistent schemes was applied to study the effect of basal texture on the mechanical behavior of magnesium alloy AZ31B sheet. The influence of the basal texture was investigated using various initial textures generated by artificially tilting the measured texture of the reference AZ31B sheet around in a transverse direction. The material parameters for the various models were fitted to experimental uniaxial tension and compression along the rolling direction and were then used to study the effects of the basal texture on the yield stress, *R* value, ultimate stress and uniform strain under uniaxial tension. The effect of the basal texture on sheet metal forming was further assessed by calculating the limit strain under in-plane plane strain tension. An assessment of the predictive capability of polycrystal plasticity models was made based on comparisons of predictions and experimental observations. Among the available self-consistent approaches, the Affine self-consistent scheme resulted in the best overall performance.

Key words: Magnesium alloys, Crystal plasticity, Twinning, Texture
doi:10.1631/jzus.A1000107 **Document code:** A **CLC number:** TG146.2

1 Introduction

There has been considerable societal and government legislative pressure on automotive producers to reduce fuel consumption and exhaust gas emissions of vehicles. One of the most effective ways to achieve this is to reduce weight by replacing steel and aluminum with magnesium in the vehicle structure and body panels. However, magnesium alloys have a number of perceived and real technological limitations, the most significant of which is their reduced formability compared to aluminum or conventional steel. This may be eliminated by the development of improved materials, or circumvented by the development of new application methods, so that these alloys can be used effectively in the volume manufacturing of lighter automobiles. However, knowledge of magnesium and its alloys is far less advanced than that of steel and aluminum. From experience of other materials like aluminum and steel, appropriate constitutive modeling is an important and necessary part of building up the knowledge of magnesium and its alloys.

Various polycrystal plasticity models have been developed for polycrystalline materials. Among them, the classic Taylor model (Taylor, 1938) has been widely used. The Taylor model assumes that all grains must accommodate the same plastic strain equal to the macroscopically imposed strain. It is well known that the Taylor assumption is reasonable for materials that show a mildly anisotropic plastic response and which are comprised of crystals with many slip systems of comparable strength. Consequently, the Taylor model works quite well for face centered cubic (FCC) and body centered cubic (BCC) materials having high crystallographic symmetries. However, the use of the

‡ Corresponding author
* Project supported by the Natural Sciences and Engineering Research Council (NSERC) Magnesium Strategic Research Network, Canada

Taylor model in other situations may lead to predictions of excessively high stresses, incorrect texture evolutions, or both (Lebensohn *et al.*, 2003). The modeling of polycrystals with a hexagonal close packed (HCP) crystallographic structure is consistent with these trends. MacEwen *et al.* (1989; 1990) have shown that the Taylor-type approach does not work well for the prediction of residual grain-interaction stresses in zirconium alloys. Muransky *et al.* (2008) and Xu *et al.* (2008) have demonstrated that the evolution of internal strains and stresses in HCP polycrystalline AZ31 and Zircaloy-2 can be predicted based on elastic-plastic self-consistent models. A self-consistent approach appears to be more suitable than the full constraint Taylor approach for constitutive modeling of HCP polycrystals.

The viscoplastic self-consistent (VPSC) model, proposed by Molinari *et al.* (1987) and Lebensohn and Tomé (1993), has been successfully applied to simulate large strain behavior and texture evolution of HCP polycrystalline Mg under various deformations (Agnew and Duygulu, 2005). Very recently, Wang *et al.* (2010a) have developed a finite strain elastic-viscoplastic self-consistent (EVPSC) model for polycrystalline materials. The EVPSC model is a completely general elastic-viscoplastic, fully anisotropic, self-consistent polycrystal model, applicable at large strains and to any crystal symmetry. They have shown that at large monotonic strains elasticity saturates and the EVPSC model gives results very close to the very popular VPSC model. For deformations involving elastoplastic transients associated with unloading and strain path changes, EVPSC predicts clear and gradual transitions, while VPSC gives stress discontinuities due to the lack of elastic deformation. It has been also demonstrated that the EVPSC model can capture some important experimental features which cannot be simulated using the VPSC model. However, Wang *et al.* (2010a) have found that numerical results based on the VPSC and EVPSC models are extremely sensitive to the stiffness of the grain-matrix interaction associated with various self-consistent schemes (SCSs) including the Secant, Affine, Tangent and the effective interaction m^{eff}. Therefore, it is necessary to carry out an assessment of the predictive capability of the VPSC/EVPSC model with various SCSs.

Various SCSs have been evaluated by comparing their predicted mechanical responses and texture evolutions with finite element calculations, full field simulations or available experimental evidence for polycrystals (e.g., Molinari and Tóth, 1994; Tomé, 1999; Lebensohn *et al.*, 2007). Note that those evaluations were based on the assumption that all the material parameters at the single crystal level are the same for various SCSs. A real challenge in modeling HCP polycrystals is that it is almost impossible to directly measure single crystal properties. Differences in stress experienced by differently orientated single crystals in an HCP polycrystal are thought to be due mainly to the orientation of a single crystal and the interaction of the single crystal with its surrounding grains, and that the interaction is sensitively dependent on the SCS employed. Therefore, for a textured HCP polycrystal, the only practical way to determine the single crystal properties in a polycrystal plasticity model is by curve-fitting numerical simulations based on the polycrystal model to the corresponding macroscopic experimental data. The predicative capability of the polycrystal plasticity model is then assessed by comparing its predictions based on the fitted material constants with the corresponding experimental data other than those used in the fitting. To the best of our knowledge, an assessment of the VPSC and EVPSC models with various SCSs has not been systematically carried out for Mg alloys. However, it is clear that such an assessment is meaningful only if the number of experiments employed is large enough to cover various different deformation processes for a given material.

In a series of studies evaluating various SCSs, Wang *et al.* (2010b) numerically studied the large strain behavior of magnesium alloy AZ31B sheet under different deformation processes. Predictions were compared with the corresponding experiments by Jain and Agnew (2007), which provided the most complete set of experimental data for Mg alloys. Values of the material parameters for the various models were fitted to experimental uniaxial tension and compression along the rolling direction (RD) and were then used to predict uniaxial tension and compression along the transverse direction (TD) and uniaxial compression in the normal direction (ND). An assessment of the predictive capability of the polycrystal plasticity models was made based on comparisons of the predicted and experimental stress

responses and R values. Wang *et al.* (2010b) concluded that, among the examined models, those with an interaction stiffness halfway between the Secant (stiff) and Tangent (compliant) give the best results. In particular, no model gives a better overall performance than the Affine self-consistent approach. While Wang *et al.* (2010b) performed the evaluation based on deformation processes that do not involve significant shear; Wang *et al.* (2010)[1] evaluated various SCSs by studying large strain homogeneous simple shear and fixed-end torsion of HCP polycrystals. They showed that the predicted second-order axial force is very sensitive to the initial texture, texture evolution and the constitutive models employed. Numerical results suggested that the torsion test can provide an effective means for assessing the adequacy of polycrystal plasticity models for HCP polycrystalline materials.

In this paper, the EVPSC model with various SCSs is further evaluated by studying the effect of the basal texture on the mechanical behavior of magnesium alloy AZ31B sheet. The study was motivated by the fact that although conventionally rolled or extruded magnesium alloys inevitably result in a dominant basal texture and thus show low formability because of the limited number of plastic deformation modes available, room temperature formability of magnesium alloys can be significantly improved through texture optimization mainly by re-orientating the basal plane. For example, Mukai *et al.* (2001) and Agnew *et al.* (2004) have shown that enhanced ductility can be achieved through equal channel angular extrusion (ECAE), where the basal planes are preferentially inclined –45° to the extrusion direction. Chino *et al.* (2008) have observed enhanced tensile ductility of AZ31 bar through torsional extrusion (TE), where the basal poles are inclined –30° to the extrusion direction. Huang *et al.* (2008) have reported an increase in the uniform strain prior to necking in AZ31 sheet produced by differential speed rolling (DSR), where the basal poles are tilted –15° in the RD. Although these shearing processes also result in significant grain refinement, which is known to enhance formability, Mukai *et al.* (2001) have been able to demonstrate that ductility is dramatically enhanced in AZ31 through texture optimization even without refining its grain structure. These experimental findings have been numerically reproduced by Wang *et al.* (2010c), who numerically assessed the influence of basal texture on the flow stress, R value and uniform strain under uniaxial tension as well as the limit strain under in-plane plane strain tension for AZ31B. However, all the simulations reported by Wang *et al.* (2010c) were based on the EVPSC model with the Affine SCS only. In the present paper, the EVPSC model with various SCSs including Secant, Affine, Tangent and the effective interaction m^{eff} is applied to study the effect of basal texture on mechanical behavior under uniaxial tension and on the limit strain under in-plane plane strain tension for magnesium alloy AZ31B sheet. An assessment of the predictive capability of the SCSs is made based on comparisons of the predictions and corresponding experimental observations. We expect that the present study and those reported by Wang *et al.* (2010b) and Wang *et al.* (2010)[1] will lead towards a comprehensive evaluation of various polycrystal plasticity models for magnesium alloys.

2 Polycrystal plasticity models

Plastic deformation of a crystal is assumed to be due to crystallographic slip and twinning on slip and twinning systems ($\boldsymbol{s}^\alpha$, $\boldsymbol{n}^\alpha$). Here, $\boldsymbol{s}^\alpha$ and $\boldsymbol{n}^\alpha$ are respectively the slip/twinning direction and normal direction of the slip/twinning system α in the present configuration. The following equation gives the grain (crystal) level plastic strain rate $\boldsymbol{d}^g$ (Asaro and Needleman, 1985):

$$\boldsymbol{d}^g = \sum_\alpha \dot{\gamma}^\alpha \boldsymbol{P}^\alpha, \tag{1}$$

where $\dot{\gamma}^\alpha$ is the shear rate of slip (twinning) on system α, and $\boldsymbol{P}^\alpha$ is the associated Schmid tensor:

$$\boldsymbol{P}^\alpha = (\boldsymbol{s}^\alpha \boldsymbol{n}^\alpha + \boldsymbol{n}^\alpha \boldsymbol{s}^\alpha)/2. \tag{2}$$

For slip,

$$\dot{\gamma}^\alpha = \dot{\gamma}_0 \left| \tau^\alpha / \tau_{\text{cr}}^\alpha \right|^{1/m} \operatorname{sgn}(\tau^\alpha), \tag{3}$$

[1] Wang, H., Wu, P.D., Neale, K.W., 2010. Numerical analysis of large strain simple shear and fixed-end torsion of HCP polycrystals. *Modelling and Simulation in Materials Science and Engineering* (submitted)

and for twinning,

$$\dot{\gamma}^{\alpha}=\begin{cases}\dot{\gamma}_0\left(\dfrac{\tau^{\alpha}}{\tau_{\mathrm{cr}}^{\alpha}}\right)^{1/m}, & \text{for } \tau^{\alpha}>0,\\ 0, & \text{for } \tau^{\alpha}\le 0,\end{cases} \tag{4}$$

where $\dot{\gamma}_0$ is a reference value of the slip/twinning rate, m is the slip/twinning rate sensitivity, and τ^{α} is the resolved shear stress defined by the product of Cauchy stress $\boldsymbol{\sigma}^g$ of grain g and $\boldsymbol{P}^{\alpha}$:

$$\tau^{\alpha}=\boldsymbol{\sigma}^g:\boldsymbol{P}^{\alpha}. \tag{5}$$

$\tau_{\mathrm{cr}}^{\alpha}$ is the critical resolved shear stress (CRSS), and sgn is the sign function. The evolution of $\tau_{\mathrm{cr}}^{\alpha}$ is taken the form of

$$\dot{\tau}_{\mathrm{cr}}^{\alpha}=\frac{\mathrm{d}\hat{\tau}^{\alpha}}{\mathrm{d}\gamma_{\mathrm{ac}}}\sum_{\beta}h^{\alpha\beta}\dot{\gamma}^{\beta}, \tag{6}$$

where $\gamma_{\mathrm{ac}}=\sum_{\alpha}|\gamma^{\alpha}|$ is the accumulated shear strain in the grain, and $h^{\alpha\beta}$ is the latent hardening coupling coefficient which empirically accounts for the obstacles on system α associated with system β. If there are k crystallographically equivalent slip/twinning modes and the ith mode has n_i slip/twinning systems, we take $h^{\alpha\beta}$ in the form of

$$h^{\alpha\beta}=\begin{bmatrix}\boldsymbol{A}_{n_1\times n_1} & q_{12}\boldsymbol{A}_{n_1\times n_2} & \cdots & q_{1k}\boldsymbol{A}_{n_1\times n_k}\\ q_{21}\boldsymbol{A}_{n_2\times n_1} & \boldsymbol{A}_{n_2\times n_2} & \cdots & q_{2k}\boldsymbol{A}_{n_2\times n_k}\\ \vdots & \vdots & & \vdots\\ q_{k1}\boldsymbol{A}_{n_k\times n_1} & q_{k2}\boldsymbol{A}_{n_k\times n_2} & \cdots & \boldsymbol{A}_{n_k\times n_k}\end{bmatrix}, \tag{7}$$

where q_{ij} is the ratio of the latent hardening rate of mode j to the self-hardening rate of mode i, and $\boldsymbol{A}_{n_i\times n_j}$ is an n_i by n_j matrix fully populated by ones. $\hat{\tau}^{\alpha}$ is the threshold stress and is characterized by

$$\hat{\tau}^{\alpha}=\tau_0^{\alpha}+(\tau_1^{\alpha}+h_1^{\alpha}\gamma_{\mathrm{ac}})\left(1-\exp\left(-\frac{h_0^{\alpha}}{\tau_1^{\alpha}}\gamma_{\mathrm{ac}}\right)\right). \tag{8}$$

Here, τ_0, h_0, h_1, and $\tau_0+\tau_1$ are the initial CRSS, the initial hardening rate, the asymptotic hardening rate, and the back-extrapolated CRSS, respectively.

Note that although we use the same symbols, such as m, $\dot{\gamma}_0$, and $\tau_{\mathrm{cr}}^{\alpha}$, for all the slip and twinning systems in the above equations, the values of these parameters are different for different slip systems and twinning systems.

Various homogenization methods have been developed to characterize the mechanical behavior of polycrystalline aggregates from the responses of their single crystals. A popular homogenizing method is the self-consistent approach, which assumes that each grain is an ellipsoidal inclusion embedded in a homogeneous effective medium (HEM), which is the aggregate of the grains. The Eshelby inclusion formalism (Eshelby, 1957), modified for incompressible media by Lebensohn *et al.* (1998), is used to describe the interaction between each grain and the aggregate. During each deformation step, the single crystal constitutive rule, which describes the grain-level response, and the self-consistency criteria are solved simultaneously. This enables the grain-level stresses and strain rates to be consistent with the boundary conditions imposed on the surrounding polycrystalline aggregate.

To apply the inclusion formalism, in connection with the non-linear viscoplastic response, first it is necessary to linearize the response. The linearized behavior of an inclusion (single crystal) can be written as

$$\boldsymbol{d}^g=\boldsymbol{M}^g:\boldsymbol{\sigma}^g+\boldsymbol{d}_0^g, \tag{9}$$

where $\boldsymbol{M}^g$ and $\boldsymbol{d}_0^g$ are the viscoplastic compliance and the back-extrapolated term of grain g, respectively. The linearized behavior of the HEM (polycrystal) is analogous to the inclusion and is written as

$$\boldsymbol{D}=\bar{\boldsymbol{M}}:\boldsymbol{\Sigma}+\boldsymbol{D}_0, \tag{10}$$

where $\bar{\boldsymbol{M}}$, $\boldsymbol{D}$, $\boldsymbol{\Sigma}$, and $\boldsymbol{D}_0$ are the viscoplastic compliance, strain rate, stress, and the back-extrapolated term of the HEM, respectively.

Different SCSs depend on different choices for the linearization. Among various SCSs, the Secant SCS employs the following linearization:

$$M_{ijkl}^{g,\text{Secant}} = \dot{\gamma}_0 \sum_{\alpha} \left(\frac{\tau^{\alpha}}{\tau_{\text{cr}}^{\alpha}} \right)^{1/m-1} \frac{P_{ij}^{\alpha} P_{kl}^{\alpha}}{\tau_{\text{cr}}^{\alpha}},$$
$$d_{0ij}^{g,\text{Secant}} = 0, \tag{11}$$

while the Affine SCS applies the linearization:

$$M_{ijkl}^{g,\text{Affine}} = \frac{\dot{\gamma}_0}{m} \sum_{\alpha} \left(\frac{\tau^{\alpha}}{\tau_{\text{cr}}^{\alpha}} \right)^{1/m-1} \frac{P_{ij}^{\alpha} P_{kl}^{\alpha}}{\tau_{\text{cr}}^{\alpha}},$$
$$d_{0ij}^{g,\text{Affine}} = \left(1 - \frac{1}{m} \right) d_{ij}^{g}. \tag{12}$$

The relation of the grain-level stress and strain rate to the aggregate response is obtained self-consistently by

$$(\boldsymbol{d}^{g} - \boldsymbol{D}) = -\tilde{\boldsymbol{M}} : (\boldsymbol{\sigma}^{g} - \boldsymbol{\Sigma}), \tag{13}$$

with the interaction tensor $\tilde{\boldsymbol{M}}$ being given by

$$\tilde{\boldsymbol{M}} = (\boldsymbol{I} - \boldsymbol{S})^{-1} : \boldsymbol{S} : \bar{\boldsymbol{M}}, \tag{14}$$

where $\boldsymbol{S}$ is the Eshelby tensor for a given grain, and $\boldsymbol{I}$ is the identity tensor.

With the aid of the Tangent and Secant relation: $\bar{\boldsymbol{M}}^{\text{Tangent}} = \bar{\boldsymbol{M}}^{\text{Secant}} / m$ (Hutchinson, 1976), the interaction tensor in the Tangent SCS is given by

$$\tilde{\boldsymbol{M}} = \frac{1}{m} (\boldsymbol{I} - \boldsymbol{S})^{-1} : \boldsymbol{S} : \bar{\boldsymbol{M}}^{\text{Secant}}. \tag{15}$$

Based on the upper and lower limits represented by the Secant and Tangent approaches, Molinari and Tóth (1994) and Tomé (1999) explored the use of an empirical adjustable parameter m^{eff}, such that $m<m^{\text{eff}}<1$. The m^{eff} scheme provides an intermediate interaction tensor:

$$\tilde{\boldsymbol{M}} = \frac{1}{m^{\text{eff}}} (\boldsymbol{I} - \boldsymbol{S})^{-1} : \boldsymbol{S} : \bar{\boldsymbol{M}}^{\text{Secant}}. \tag{16}$$

A comprehensive discussion of the different linearization procedures can be found in Lebensohn *et al.* (2007).

Several twinning models have been developed (Tomé *et al.*, 1991; Staroselsky and Anand, 1998; Proust *et al.*, 2009; Beyerlein and Tomé, 2010). The predominant twin reorientation (PTR) scheme proposed by Tomé *et al.* (1991) is the most popular and is used in this study to model the reorientation by twinning. PTR prevents grain reorientation by twinning until a threshold value A^{th1} is accumulated in any given system and rapidly raises the threshold to a value around $A^{\text{th1}}+A^{\text{th2}}$.

For simplicity, EVPSC models with Affine, Secant, Tangent, and m^{eff} SCSs are respectively called the Affine, Secant, Tangent, and meff models in the rest of this paper.

3 Results

An assessment of the predicative capability of a polycrystal plasticity model is meaningful only if the number of experiments employed is large enough to cover various different deformation processes for a given material. The Mg alloy with the most complete set of experimental data is the AZ31B sheet studied by Jain and Agnew (2007). Therefore, this material was the reference sheet (or 'as received' sheet) in the present study. The initial texture in terms of the {00.1} and {10.0} pole figures is shown in Fig. 1. It is a typical rolling texture with major and minor peaks close to the ND, at about 5° and −5° along the RD, respectively. Fig. 1 also shows the textures obtained by rotating the reference texture by an angle α about the TD. In the {00.1} pole figures, this rotation results in a vertical downward translation of the peaks in the reference texture (i.e., a downward translation of the peaks along RD). The intensity of the basal texture as a function of the tilt angle α is shown in Fig. 2. The intensity is calculated as the ratio of the number of grains with a maximum orientational difference from the ideal basal orientation of less than 15°, to the total number of grains. The ideal grain orientation corresponds to a perfect alignment of the basal pole with the ND. The intensity decreases rapidly when the tilt angle is relatively large. Note that the calculated intensity for α=5° is higher than for α=0° (reference texture). The reason is that the reference texture has its major peak at around 5° with respect to the RD. For α=5°, this peak is translated into the centre of the pole figure (i.e., the ideal orientation), resulting in the observed intensification of the basal texture.

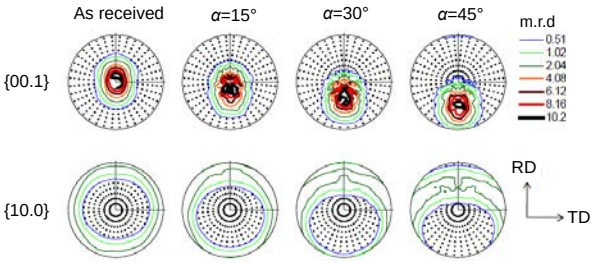

Fig. 1 Initial textures represented in terms of the {00.1} and {10.0} pole figures
The 'as received' texture is the measured initial texture of the reference sheet. The others are obtained by artificially rotating α degrees the reference texture around the TD towards the opposite direction of the RD. m.r.d represents the multiples of a random distribution

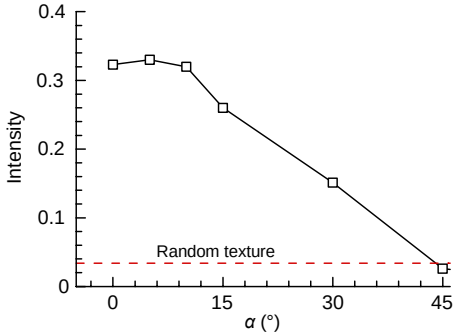

Fig. 2 Intensity of basal texture as a function of tilt angle α

Following Wang *et al.* (2010c), plastic deformation of AZ31B sheet is due to the basal $\langle a\rangle(\{0001\}\langle 11\bar{2}0\rangle)$, prismatic $\langle a\rangle(\{10\bar{1}0\}\langle 11\bar{2}0\rangle)$, and pyramidal $\langle c+a\rangle(\{\bar{1}\bar{1}22\}\langle\bar{1}\bar{1}23\rangle)$ slip systems, and the $\{10\bar{1}2\}\langle\bar{1}011\rangle$ tensile twin system (Fig. 3). We assume that the reference slip/twinning rate $\dot{\gamma}_0$ and rate sensitivity m are the same for all slip/twinning systems, and are taken as $\dot{\gamma}_0$=0.001 s^{-1} and m=0.05, respectively. These values are typical for magnesium alloys. We further assume that there are no latent hardening effects between slip systems, i.e., q_{ij}=1 for i, j=1, 2, 3. Values of the other material parameters in the EVPSC model with various SCSs were estimated by curve-fitting numerical simulations of uniaxial tension and compression along the RD to the corresponding experimental data. Note that tensile twinning occurs rarely during uniaxial tension within the plane of a sheet with a strong basal texture. Uniaxial tension thus allows us to independently fit the material parameters associated with the slip systems. The material parameters related to the tensile twinning can be determined by uniaxial compression along the RD, where tensile twinning is the predominant plastic deformation mode at small strains. Fig. 4 shows the uniaxial tension and compression true stress and true plastic strain curves along the RD. All the models employed could reasonably fit the experimental curves, and the importance of twinning in compression is clearly revealed by the characteristic S-shape of the flow curves. The determined values of the material constants are listed in Table 1, where q_{i4} represents the latent hardening effect between a slip/twining system (i=1, basal slip; i=2, prismatic slip; i=3, pyramidal slip; i=4, tensile twinning).

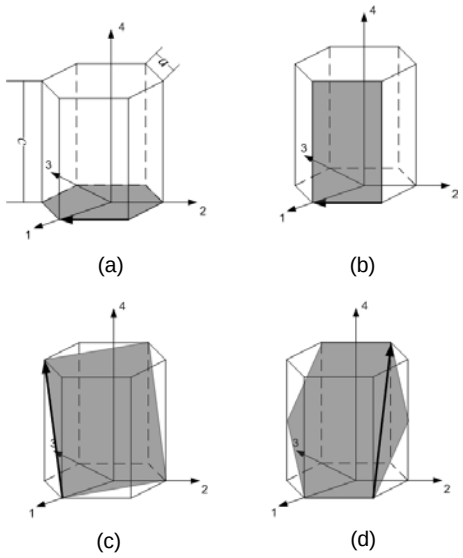

Fig. 3 Plastic deformation modes in hexagonal structure
(a) Basal $\langle a\rangle$ slip systems; (b) Prismatic $\langle a\rangle$ slip systems; (c) Pyramidal $\langle c+a\rangle$ slip systems; (d) Tensile twin (Wang *et al.*, 2010a)

We proceeded by numerically predicting the effect of the basal texture on uniaxial tension along the RD, using the polycrystal plasticity models and the corresponding values of material parameters determined above. Fig. 5 shows the predicted engineering stress-engineering strain curves under uniaxial tension along the RD based on various models for the four initial textures shown in Fig. 1. The symbol shown in Fig. 5 indicates the necking or uniform strain, the strain corresponding to the maximum engineering stress. All the models predicted a general trend: the influence of tensile twinning increases with tilt angle α.

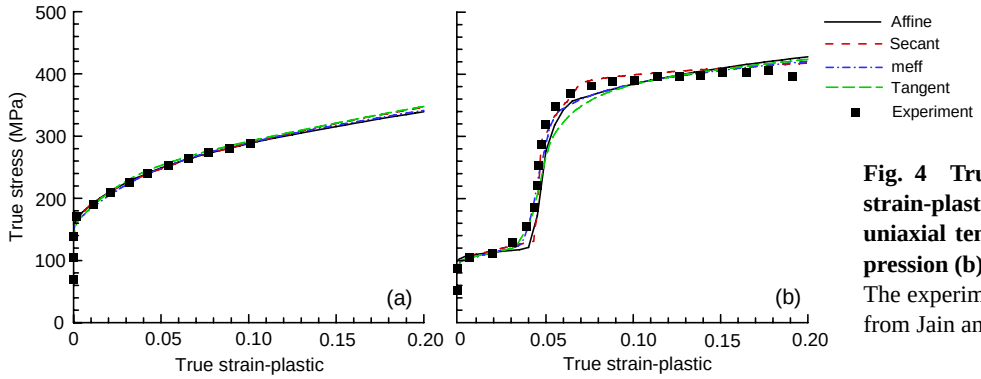

Fig. 4 True stress and true strain-plastic curves under uniaxial tension (a) and compression (b) along the RD
The experimental data are taken from Jain and Agnew (2007)

Table 1 Material constants for various self-consistent models

Model	Mode	τ_0	τ_1	h_0	h_1	q_{i4}	A^{th1}	A^{th2}
Affine	Basal	9	1	5000	25	4		
	Prismatic	79	40	590	50	4		
	Pyramidal	100	100	5000	0	2		
	Tensile twin	47	0	0	0	4	0.72	0
Secant	Basal	13	4	5000	30	4		
	Prismatic	73	35	400	60	4		
	Pyramidal	110	83	2500	0	2		
	Tensile twin	31	0	0	0	4	0.82	0
meff (m^{eff}=0.1)	Basal	17	6	3800	100	4		
	Prismatic	77	33	650	50	4		
	Pyramidal	148	35	9600	0	2		
	Tensile twin	33	0	0	0	4	0.81	0
Tangent	Basal	21	5	3000	140	4		
	Prismatic	90	15	580	70	4		
	Pyramidal	145	30	9600	0	2		
	Tensile twin	38	0	0	0	4	0.81	0

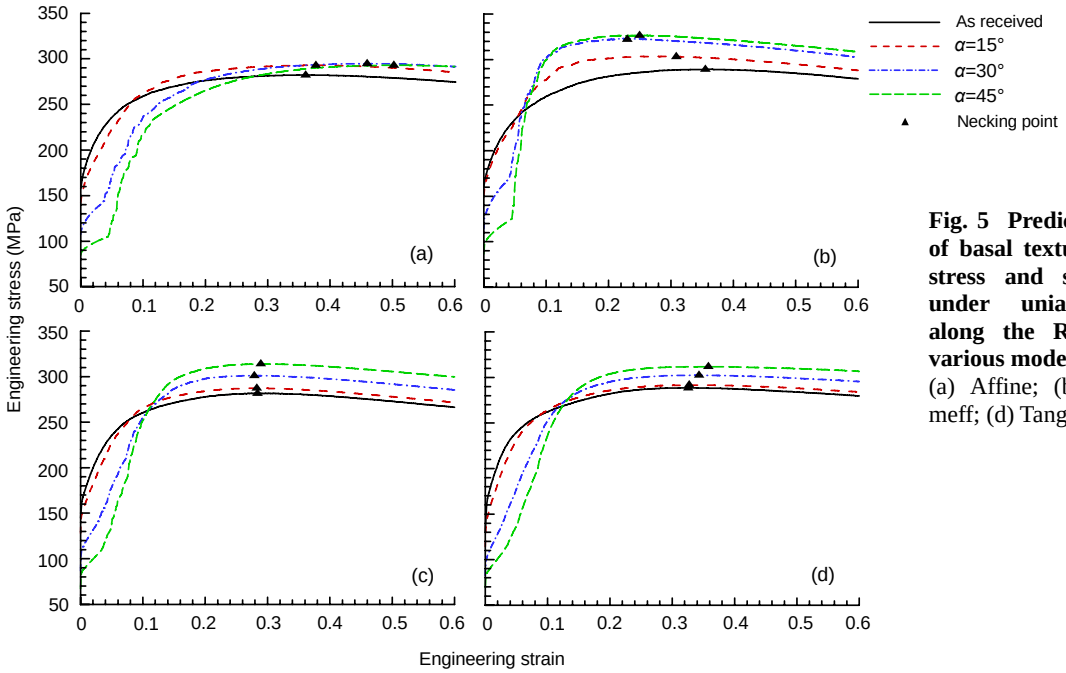

Fig. 5 Predicted influence of basal texture on tensile stress and strain curves under uniaxial tension along the RD based on various models
(a) Affine; (b) Secant; (c) meff; (d) Tangent

The predicted influence of the basal texture on the mechanical behavior of magnesium alloy AZ31B under uniaxial tension can be more clearly demonstrated in terms of variations in yield stress σ_y (Fig. 6a), ultimate stress σ_u (Fig. 6b) and uniform strain ε_u (Fig. 6c) with respect to the tilt angle α. All the models predicted that increasing the tilt angle α decreases the yield stress σ_y. Fig. 6b shows that the calculated ultimate stress σ_u monotonically increases with α based on the Secant, meff and Tangent models. The results from the Affine model indicate that the ultimate stress σ_u increases with α up to a maximum at α=30°, then decreases slightly. The predicted effect of the basal texture on the uniform strain ε_u is sensitively dependent on the polycrystal plasticity models (Fig. 6c). More specifically, a monotonic increase in uniform strain ε_u with respect to the tilt angle α was found to be very significant in the Affine model but very small in the Tangent model. The calculated uniform strain ε_u is almost independent of the tilt angle α if the meff model is used. The results according to the Secant model indicate that the uniform strain ε_u even decreases rapidly with α down to a minimum at α=30°, and then increases slightly.

The so-called *R* value, defined as the transverse-to-thickness plastic strain-ratio under uniaxial tension within the sheet plane, is often used to characterize the anisotropy of the sheet in the sheet metal industry. The measured *R* values are often used to calculate material parameters involved in anisotropic yield functions (Wu *et al.*, 2003; Barlat *et al.*, 2007). Here, the prediction of *R* values will provide an independent test of the validity of each model. Fig. 7 shows the predicted *R* value vs. imposed strain curves under uniaxial tension along the RD. All the models showed general trends: the *R* value dramatically decreases with an increasing tilt angle and the *R* value evolves significantly with straining. Comparing the predicted and measured *R* values for the "as received" sheet (α=0°) at the strain ε=0.11 indicates that the Secant model grossly overestimates the *R* value. The results based on the Affine and meff models slightly overestimate the *R* value, while the Tangent model underestimates *R* slightly. The measured *R* values are often used to calculate material parameters involved in anisotropic yield functions. These anisotropic yield functions are such that *R* is often assumed to be constant with strain. This assumption is reasonable in the yield functions designed for FCC and BCC polycrystalline sheets because variations in *R* values with applied deformation are relatively small (Barlat *et al.*, 2007). However, for HCP materials, such as the magnesium alloy AZ31B sheet in this study, the predicted *R* value evolves significantly with straining. Note that the variation in *R* value with imposed tensile straining shown in Fig. 7 is supported by experimental results from studies of magnesium alloys at room temperature (Avery *et al.*, 1965; Kaiser *et al.*, 2003; Agnew and Duygulu, 2005; Hartig *et al.*, 2005; Lou *et al.*, 2007; del Valle and Ruano, 2009). Therefore, Fig. 7 clearly indicates that the assumption of a constant in-plane *R* value under uniaxial tension for determining material constants in anisotropic yield functions for HCP polycrystalline sheets is not appropriate (Wang *et al.*, 2010b).

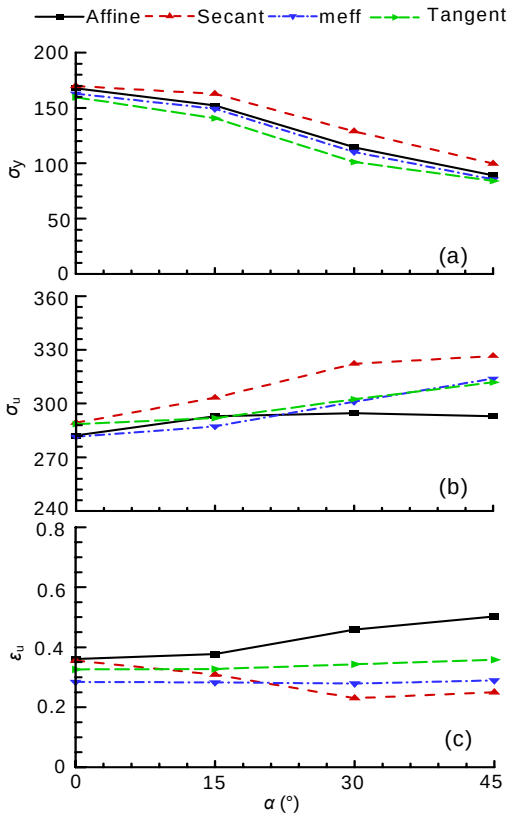

Fig. 6 Predicted influence of basal texture on yield stress σ_y (a), ultimate stress σ_u (b), and uniform strain ε_u (c) based on various models

For a sheet under uniaxial tension at tensile plastic strain ε^p, the plastic strains in the transverse and thickness directions are $-R\varepsilon^p/(1+R)$ and

$-\varepsilon^{p}/(1+R)$, respectively. A smaller R value thus implies a larger accommodation of the imposed deformation in the thickness direction than in the transverse direction. Fig. 7 suggests that the influence of the basal texture on the formability of sheet under biaxial tension (i.e., the in-plane minimum principal strain is non-negative) is more significant than that under uniaxial tension. Therefore, the influence of the basal texture on the limit strain of sheet under in-plane plane strain tension was also studied in the context of the forming limit diagram (FLD). Following the numerical procedure developed by Wu *et al.* (1997), the EVPSC model with various SCSs, in conjunction with the M-K approach proposed by Marciniak and Kuczynski (1967), was implemented into a numerical code for constructing the FLDs (Wang *et al.*, 2010)[2]. The basic assumption of the M-K approach is the existence of material imperfections in the form of grooves on the surface of the sheet. It was shown that a slight intrinsic inhomogeneity in load bearing capacity throughout a deforming sheet can lead to unstable growth of strain in the region of the imperfection, and subsequently cause localized necking and failure.

Although the numerical procedure employed is able to calculate the entire FLD under proportional loading ($-0.5\leq(D_{22}/D_{11})\leq 1$, D_{ij} are components of macroscopic strain rate $\boldsymbol{D}$ in Eq. (10)) (Wu *et al.*, 1998; 2004b) and effects of strain path changes on FLDs (Wu *et al.*, 2005), here we studied only the limit strain under in-plane plane strain tension, in which the deformation outside the imperfection band was assumed to be such that $D_{22}=0$, $D_{12}=0$, $W_{12}=0$. The initial geometric non-uniformity was assumed to be $f_0=0.99$.

Fig. 8 shows the predicted effect of the basal texture on the limit strain under in-plane plane strain tension. The predicted formability based on all the models was found to be dramatically enhanced by tilting the basal orientation away from ND around TD. Note that the Secant model presented a rapid decrease in uniform and necking strain due to the tilt angle α. Furthermore, comparing Figs. 6c and 8 reveals that the effect of the basal texture on the limit strain under stretching is much more significant than that on the uniform strain under uniaxial tension.

[2] Wang, H., Wu, P.D., Boyle, K.P., Neale, K.W., 2010. On crystal plasticity formability analysis for magnesium alloy sheets. *International Journal of Solids and Structures* (submitted)

4 Discussion and conclusions

In this paper, the effect of the basal texture on the mechanical behaviour of AZ31B sheet was studied using the EVPSC model with various SCSs. The material parameters for the various models were fitted to experimental uniaxial tension and compression curves along the RD. The effect of the basal texture was investigated using various initial textures generated by artificially tilting the measured texture of conventional AZ31B sheet around TD. Numerical results suggested that:

1. The influence of tensile twinning increases with increasing tilt angle in all the models.

2. The yield stress σ_y under uniaxial tension decreases with increasing tilt angle in all the models.

3. The ultimate stress σ_u under uniaxial tension increases with increasing tilt angle in all the models.

4. The R value under uniaxial tension decreases with increasing tilt angle in all the models.

5. The limit strain ε_l under in-plane plane strain tension increases dramatically with increasing tilt angle in all the models.

6. The uniform strain ε_u could be either raised or lowered with increasing tilt angle α, depending on the SCSs employed: (1) ε_u significantly increases with α in the Affine model; (2) ε_u slightly increases with α in the Tangent model; (3) ε_u is almost independent of α in the meff model; (4) ε_u rapidly decreases with α in the Secant model.

Experiments have clearly shown that the uniform strain under uniaxial tension can be significantly improved through texture optimization mainly by re-orientating the basal plane. Based on comparisons of the predicted and experimentally observed uniform strain under uniaxial tension, our results confirm that the EVPSV model with the Affine self-consistent scheme gives the best performance (Wang *et al.*, 2010b).

The current polycrystal plasticity models with both slip and twinning, including EVPSC, VPSC and the models developed by Kalidindi (2001) and Wu P.D. *et al.* (2007), involve a large number of fitting parameters, which may not be uniquely determined. Therefore, to some extent, the predictive capability of such polycrystal plasticity models relies on introducing more constraints such that the number of suitable parameter combinations can be significantly

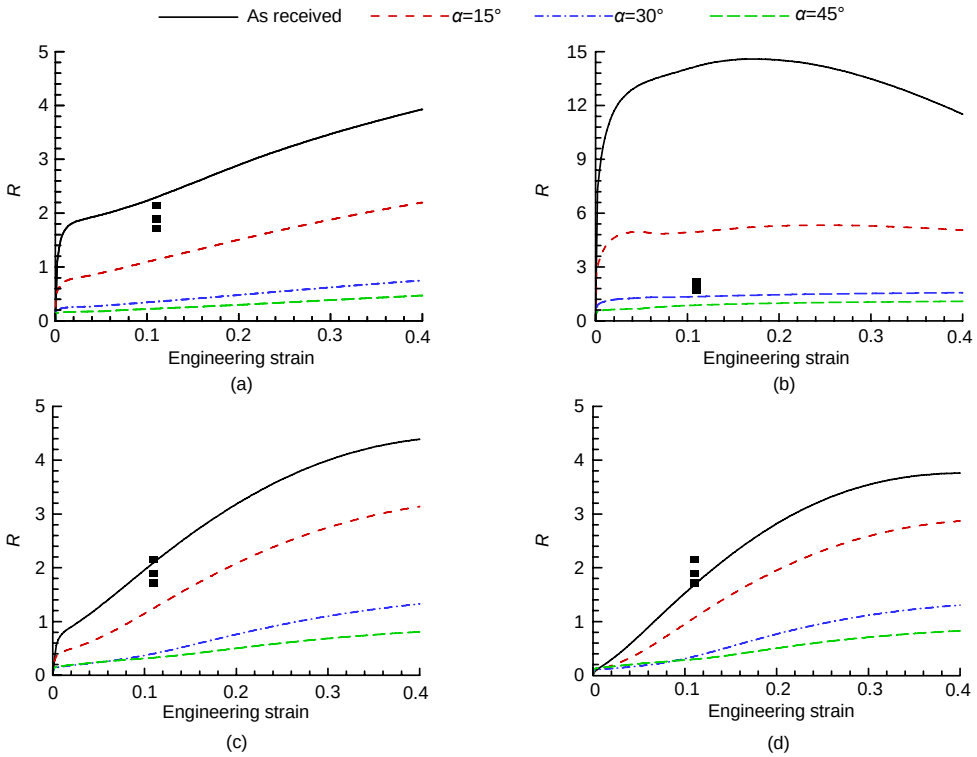

Fig. 7 Predicted influence of basal texture on *R* value vs. strain curves under uniaxial tension along the RD based on various models. (a) Affine; (b) Secant; (c) meff; (d) Tangent. Solid squares are the experimental *R* values at tensile strain for the "as received" sheet taken from Agnew and Duygulu (2005) and Jain and Agnew (2007)

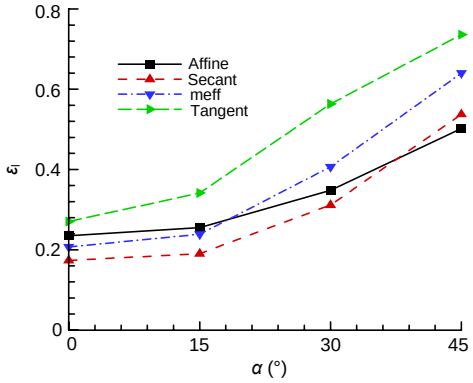

Fig. 8 Predicted influence of basal texture on limit strain ε_l under in-plane plane strain tension based on various models

reduced. It is accepted that the evolution of elastic lattice strains during loading in different grain orientations can be used as a very sensitive indicator of plastic deformation mechanisms at microscopic levels. Therefore, an efficient way to do so is to obtain the material parameters by not only fitting the macroscopic stress-strain curves and deformation textures, but also simultaneously fitting elastic lattice strains measured by in situ neutron diffraction. This work is in progress.

Finally, the validity of a polycrystal plasticity model can be assessed by comparing numerical results predicted by the polycrystal plasticity theory with the corresponding finite element (FE) crystal plasticity simulation. In FE simulations an element of the FE mesh represents either a single crystal or a part of a single crystal, and the constitutive response at an integration point is described by the single crystal constitutive model. This approach enforces both equilibrium and compatibility throughout the polycrystalline aggregate in the weak FE sense (Anand and Kalidindi, 1994; Wu *et al.*, 2004a). Furthermore, it facilitates consideration of grain morphology and the modeling of localized deformations in single and polycrystals (Wu *et al.*, 2006; Wu X. *et al.*, 2007; Shi *et al.*, 2010). This work is also in progress.

References

Agnew, S.R., Duygulu, O., 2005. Plastic anisotropy and the role of non-basal slip in magnesium alloy AZ31B. *International Journal of Plasticity*, **21**(6):1161-1193. [doi:10. 1016/j.ijplas.2004.05.018]

Agnew, S.R., Horton, J.A., Lillo, T.M., Brown, D.W., 2004. Enhanced ductility in strongly textured magnesium produced by equal channel angular processing. *Scripta Materialia*, **50**(3):377-381. [doi:10.1016/j.scriptamat.2003.10.006]

Anand, L., Kalidindi, S.R., 1994. The process of shear band formation in plane strain compression of fcc metals: effects of crystallographic texture. *Mechanics of Materials*, **17**(2-3):223-243. [doi:10.1016/0167-6636(94)90062-0]

Asaro, R.J., Needleman, A., 1985. Texture development and strain hardening in rate dependent polycrystals. *Acta Metallurgica et Materialia*, **33**:923-953.

Avery, D.H., Hosford, W.F., Backofen, W.A., 1965. Plastic anisotropy in magnesium alloy sheets. *Transactions of the Metallurgical Society of AIME*, **233**:71-78.

Barlat, F., Yoon, J.W., Cazacu, O., 2007. On linear transformation based anisotropic yield functions. *International Journal of Plasticity*, **23**(5):876-896. [doi:10.1016/j.ijplas.2006.10.001]

Beyerlein, I.J., Tomé, C.N., 2010. A probabilistic twin nucleation model for HCP polycrystalline metals. *Proceedings of the Royal Society A: Mathematical Physical & Engineering Sciences*, **466**(2121):2517. [doi:10.1098/rspa.2009.0661]

Chino, Y., Sassa, K., Mabuchi, M., 2008. Enhancement of tensile ductility of magnesium alloy produced by torsion extrusion. *Scripta Materialia*, **59**(4):399-402. [doi:10.1016/j.scriptamat.2008.04.013]

del Valle, J.A., Ruano, O.A., 2009. Effect of annealing treatments on the anisotropy of a magnesium alloy sheet processed by severe rolling. *Materials Letters*, **63**(17):1551-1554. [doi:10.1016/j.matlet.2009.04.014]

Eshelby, J.D., 1957. The determination of the elastic field of an ellipsoidal inclusion, and related problems. *Proceedings of the Royal Society of London. Series A, Mathematical and Physical Sciences*, **241**(1226):376-396.

Hartig, Ch., Styczynski, A., Kaiser, F., Letzig, D., 2005. Plastic anisotropy and texture evolution of rolled AZ31 magnesium alloys. *Materials Science Forum*, **495-497**:1615-1620. [doi:10.4028/www.scientific.net/MSF.495-497.1615]

Huang, X.S., Suzuki, K., Watazu, A., Shigematsu, I., Saito, N., 2008. Mechanical properties of Mg-Al-Zn alloy with a tilted basal texture obtained by differential speed rolling. *Materials Science and Engineering: A*, **488**(1-2): 214-220. [doi:10.1016/j.msea.2007.11.029]

Hutchinson, J.W., 1976. Bounds and self-consistent estimates for creep of polycrystalline materials. *Proceedings of the Royal Society of London. Series A, Mathematical and Physical Sciences*, **348**(1652):101-127.

Jain, A., Agnew, S.R., 2007. Modeling the temperature dependent effect of twinning on the behavior of magnesium alloy AZ31B sheet. *Materials Science and Engineering: A*, **462**(1-2):29-36. [doi:10.1016/j.msea.2006.03.160]

Kaiser, F., Letzig, D., Bohlen, J., Styczynski, A., Hartig, Ch., Kainer, K.U., 2003. Anisotropic properties of magnesium sheet AZ31. *Materials Science Forum*, **419-422**:315-320. [doi:10.4028/www.scientific.net/MSF.419-422.315]

Kalidindi, S.R., 2001. Modeling anisotropic strain hardening and deformation textures in low stacking fault energy fcc metals. *International Journal of Plasticity*, **17**(6):837-860. [doi:10.1016/S0749-6419(00)00071-1]

Lebensohn, R.A., Tomé, C.N., 1993. A self-consistent anisotropic approach for the simulation of plastic deformation and texture development of polycrystals: Application to zirconium alloys. *Acta Metallurgica et Materialia*, **41**(9):2611-2624. [doi:10.1016/0956-7151(93)90130-K]

Lebensohn, R.A., Turner, P.A., Signorelli, J.W., Canova, G.R., Tomé, C.N., 1998. Calculation of intergranular stresses based on a large strain visco-plastic self-consistent model. *Modelling and Simulation in Materials Science and Engineering*, **6**(4):447-465. [doi:10.1088/0965-0393/6/4/011]

Lebensohn, R.A., Dawson, P.R., Kern, H.M., Wenk, H.R., 2003. Heterogeneous deformation and texture development in halite polycrystals: comparison of different modeling approaches and experimental data. *Tectonophysics*, **370**(1-4):287-311. [doi:10.1016/S0040-1951(03)00192-6]

Lebensohn, R.A., Tomé, C.N., Castañeda, P.P., 2007. Self-consistent modeling of the mechanical behavior of viscoplastic polycrystals incorporating intragranular field fluctuations. *Philosophical Magazine*, **87**(28):4287-4322. [doi:10.1080/14786430701432619]

Lou, X.Y., Li, M., Boger, R.K., Agnew, S.R., Wagoner, R.H., 2007. Hardening evolution of AZ31B Mg sheet. *International Journal of Plasticity*, **23**(1):44-86. [doi:10.1016/j.ijplas.2006.03.005]

MacEwen, S.R., Tomé, C., Faber, J., 1989. Residual-stresses in annealed zircaloy. *Acta Metallurgica*, **37**(3):979-989. [doi:10.1016/0001-6160(89)90025-4]

MacEwen, S.R., Christodoulou, N., Salinasrodriguez, A., 1990. Residual grain-interaction stresses in zirconium alloys. *Metallurgical Transactions*, **21A**:1083-1095.

Marciniak, Z., Kuczynski, K., 1967. Limit strains in the process of stretch-forming sheet metal. *International Journal of Mechanical Sciences*, **9**(9):609-620. [doi:10.1016/0020-7403(67)90066-5]

Molinari, A., Tóth, L.S., 1994. Tuning a self-consistent viscoplastic model by finite element results. Part I: Modeling. *Acta Metallurgica et Materialia*, **42**(7):2453-2458. [doi:10.1016/0956-7151(94)90324-7]

Molinari, A., Canova, G.R., Ahzi, S., 1987. A self-consistent approach of the large deformation polycrystal viscoplasticity. *Acta Metallurgica*, **35**(12):2983-2994. [doi:10.1016/0001-6160(87)90297-5]

Mukai, T., Yamanoi, M., Watanabe, H., Higashi, K., 2001. Ductility enhancement in AZ31 magnesium alloy by controlling its grain structure. *Scripta Materialia*, **45**(1):89-94. [doi:10.1016/S1359-6462(01)00996-4]

Muransky, O., Carr, D.G., Barnett, M.R., Oliver, E.C., Sittner, P., 2008. Investigation of deformation mechanisms involved in the plasticity of AZ31 Mg alloy: in situ neutron diffraction and EPSC modelling. *Materials Science and Engineering: A*, **496**(1-2):14-24. [doi:10.1016/j.msea.2008.07.031]

Proust, G., Tomé, C.N., Jain, A., Agnew, S.R., 2009. Modeling the effect of twinning and detwinning during strain-path changes of magnesium alloy AZ31. *International Journal of Plasticity*, **25**(5):861-880. [doi:10.1016/j.ijplas.2008.05.005]

Shi, Y., Wu, P.D., Lloyd, D.J., Embury, J.D., 2010. Crystal plasticity based analysis of localized necking in aluminum tube under internal pressure. *European Journal of Mechanics A/Solids*, **29**(4):475-483. [doi:10.1016/j.euromechsol.2010.03.005]

Staroselsky, A., Anand, L., 1998. Inelastic deformation of F.C.C. materials by slip and twinning. *Journal of the Mechanics and Physics of Solids*, **46**(4):671-696. [doi:10.1016/S0022-5096(97)00071-9]

Taylor, G.I., 1938. Plastic strain in metals. *Journal of the Institute of Metals*, **62**:307-324.

Tomé, C.N., 1999. Self-consistent polycrystal models: a directional compliance criterion to describe grain interactions. *Modeling and Simulation in Material Science Engineering*, **7**(5):723-738. [doi:10.1088/0965-0393/7/5/305]

Tomé, C.N., Lebensohn, R.A., Kocks, U.F., 1991. A model for texture development dominated by deformation twinning-application to zirconium alloys. *Acta Metallurgica et Materialia*, **39**(11):2667-2680. [doi:10.1016/0956-7151(91)90083-D]

Wang, H., Wu, P.D., Tomé, C.N., Huang, Y., 2010a. A finite strain elastic-viscoplastic self-consistent model for polycrystalline materials. *Journal of the Mechanics and Physics of Solids*, **58**(4):594-612. [doi:10.1016/j.jmps.2010.01.004]

Wang, H., Raeisinia, B., Wu, P.D., Agnew, S.R., Tomé, C.N., 2010b. Evaluation of self-consistent crystal plasticity models for magnesium alloy AZ31B sheet. *International Journal of Solids and Structures*, **47**(21):2905-2917. [doi:10.1016/j.ijsolstr.2010.06.016]

Wang, H., Wu, P.D., Gharghouri, M.A., 2010c. Effects of basal texture on mechanical behaviour of magnesium alloy AZ31 sheet. *Materials Science and Engineering: A*, **527**(15):3588-3594. [doi:10.1016/j.msea.2010.02.050]

Wu, P.D., Neale, K.W., van der Giessen, E., 1997. On crystal plasticity FLD analysis. *Proceedings of the Royal Society of London. Series A, Mathematical, Physical and Engineering Sciences*, **453**(1964):1831-1848. [doi:10.1098/rspa.1997.0099]

Wu, P.D., Neale, K.W., van der Giessen, E., Jain, M., Makinde, A., MacEwen, S.R., 1998. Crystal plasticity forming limit diagram analysis of rolled aluminum sheets. *Metallurgical and Materials Transactions A*, **29**(2):527-535. [doi:10.1007/s11661-998-0134-x]

Wu, P.D., Jain, M., Savoie, J., MacEwen, S.R., Tugcu, P., Neale, K.W., 2003. Evaluation of anisotropic yield functions for aluminum sheets. *International Journal of Plasticity*, **19**(1):121-138. [doi:10.1016/S0749-6419(01)00033-X]

Wu, P.D., MacEwen, S.R., Lloyd, D.J., Neale, K.W., 2004a. A mesoscopic approach for predicting sheet metal formability. *Modelling and Simulation in Materials Science and Engineering*, **12**(3):511-527. [doi:10.1088/0965-0393/12/3/011]

Wu, P.D., MacEwen, S.R., Lloyd, D.J., Neale, K.W., 2004b. Effect of cube texture on sheet metal formability. *Materials Science and Engineering: A*, **364**(1-2):182-187. [doi:10.1016/j.msea.2003.08.020]

Wu, P.D., Graf, A., MacEwen, S.R., Lloyd, D.J., Jain, M., Neale, K.W., 2005. On forming limit stress diagram analysis. *International Journal of Solids and Structures*, **42**(8):2225-2241. [doi:10.1016/j.ijsolstr.2004.09.010]

Wu, P.D., Huang, Y., Lloyd, D.J., 2006. Studying grain fragmentation in ECAE by simulating simple shear. *Scripta Materialia*, **54**(12):2107-2112. [doi:10.1016/j.scriptamat.2006.03.016]

Wu, P.D., Lloyd, D.J., Jain, M., Neale, K.W., Huang, Y., 2007. Effects of spatial grain orientation distribution and initial surface topography on sheet metal necking. *International Journal of Plasticity*, **23**(6):1084-1104. [doi:10.1016/j.ijplas.2006.11.005]

Wu, X., Kalidindi, S.R., Necker, C., Salem, A.A., 2007. Prediction of crystallographic texture evolution and anisotropic stress-strain curves during large plastic strains in high purity α-titanium using a Taylor-type crystal plasticity model. *Acta Materialia*, **55**(2):423-432. [doi:10.1016/j.actamat.2006.08.034]

Xu, F., Holt, R.A., Daymond, M.R., 2008. Modeling lattice strain evolution during uniaxial deformation of textured Zircaloy-2. *Acta Materialia*, **56**(14):3672-3687. [doi:10.1016/j.actamat.2008.04.019]